Original Article

MOLECULAR METABOLISM

SERPINA3C ameliorates adipose tissue inflammation through the Cathepsin G/Integrin/AKT pathway

Bai-Yu Li [1], Ying-Ying Guo [1], Gang Xiao [1], Liang Guo [2,], Qi-Qun Tang [1,*]**

ABSTRACT

Objective: Due to the increasing prevalence of obesity and insulin resistance, there is an urgent need for better treatment of obesity and its related metabolic disorders. This study aimed to elucidate the role of SERPINA3C, an adipocyte secreted protein, in obesity and related metabolic disorders.

Methods: Male wild type (WT) and knockout (KO) mice were fed with high-fat diet (HFD) for 16 weeks, adiposity, insulin resistance, and inflammation were assessed. AAV-mediated overexpression of SERPINA3C was injected locally in inguinal white adipose tissue (iWAT) to examine the effect of SERPINA3C. *In vitro* analyses were conducted in 3T3-L1 adipocytes to explore the molecular pathways underlying the function of SERPINA3C.

Results: Functional exploration of the SERPINA3C knockout mice revealed that SERPINA3C deficiency led to an impaired metabolic phenotype (more severe obesity, lower metabolic rates, worse glucose intolerance and insulin insensitivity), which was associated with anabatic inflammation and apoptosis of white adipose tissues. Consistent with these results, overexpression of SERPINA3C in inguinal adipose tissue protected mice against diet-induced obesity and metabolic disorders with less inflammation and apoptosis in adipose tissue. Mechanistically, SERPINA3C inhibited Cathepsin G activity, acting as a serine protease inhibitor, which blocked Cathepsin G-mediated turnover of $\alpha 5/\beta 1$ Integrin protein. Then, the preserved integrity (increase) of $\alpha 5/\beta 1$ Integrin signaling activated AKT to decrease JNK phosphorylation, thereby inhibiting inflammation and promoting insulin sensitivity in adipocytes.

Conclusions/interpretation: These findings demonstrate a previously unknown SERPINA3C/Cathepsin G/Integrin/AKT pathway in regulating adipose tissue inflammation, and suggest the therapeutic potential of targeting SERPINA3C/Cathepsin G axis in adipose tissue for the treatment of obesity and metabolic diseases.

Keywords Insulin resistance; Inflammation; White adipose tissue; Adipokine; Integrin $\alpha 5/\beta 1$

1. INTRODUCTION

Obesity, which has become a serious health problem worldwide, is associated with chronic inflammation that may cause the development of insulin resistance and its common comorbidity, type 2 diabetes [1]. Insulin resistance arises from the inability of insulin to act normally in regulating glucose homeostasis in peripheral tissues. Inflammation in the white adipose tissue (WAT) plays an active role in morbid obesity. In an environment of caloric excess, expansion of adipose tissue can trigger chronic, low-grade inflammation and adipocyte cell death, which ultimately result in insulin resistance [2]. To date, several pathways have been studied for the treatment of obesity and related diseases, including adipose tissue browning [3—5], exercise [6—9], and the use of adipokines [10]. Adipokines are adipose tissue-secreted proteins that regulate adipose tissue and systemic metabolism, acting through autocrine/paracrine and endocrine signaling to regulate cell functions, peripheral insulin actions, and glucose homeostasis [11]. Changes in adipokine secretion occur in obesity and other conditions characterized by insulin resistance such as type 2 diabetes [12], suggesting the roles of adipokine dysregulation in the initiation and progression of metabolic diseases.

The serine protease inhibitor (serpin) superfamily is the largest group of protease inhibitors in nature [13,14]. A phylogenetic study of the superfamily divided the eukaryotic serpins into 16 "clades" (termed A—P). The proteins are named SERPINXy, where X is the clade and y is the number within that clade [15]. Serpins can target and inactivate multiple serine proteases, including thrombin, chymotrypsin, Cathepsin G, and neutrophil elastase [16,17]. In the classic serpin "conformational trapping" mechanism of inhibition, cleavage of the reactive center loop (RCL) by the target protease allows structural

[1]Key Laboratory of Metabolism and Molecular Medicine of the Ministry of Education, Department of Biochemistry and Molecular Biology of School of Basic Medical Sciences and Department of Endocrinology and Metabolism of Zhongshan Hospital, Fudan University, Shanghai, 200032, China [2]School of Kinesiology, and Shanghai Frontiers Science Research Base of Exercise and Metabolic Health, Shanghai University of Sport, Shanghai, 200438, China

*Corresponding author. E-mail: qqtang@shmu.edu.cn (Q.-Q. Tang).

**Corresponding author. E-mail: guoliang@sus.edu.cn (L. Guo).

Received March 11, 2022 • Revision received April 10, 2022 • Accepted April 13, 2022 • Available online 15 April 2022

https://doi.org/10.1016/j.molmet.2022.101500

conversion by rapid opening of β-sheet A and insertion of the cleaved RCL as an additional strand. The target protease remains covalently bound to the RCL and loses its enzymatic activity [13]. Because of their molecular flexibility and anti-protease activity, serpins play important roles in the biochemical and biological functions of the human body, and control proteolytic pathways related to human health and diseases. Among 16 phylogenetic clades, SERPINA3C belongs to the secretory clade A serpins. A previous report indicated that, during 3T3-L1 adipogenesis, SERPINA3C played an important role in the transition of 3T3-L1 cells from mitotic clonal expansion to terminal differentiation, and was critical for adipocyte differentiation [18]. An Apoe$^{-/-}$/SERPINA3C$^{-/-}$ double-knockout mouse model was used to discover the protective role of SERPINA3C against atherosclerosis after high-fat diet (HFD) feeding [19]. Although studies have shown the protective role of SERPINA3C in some murine diseases [19,20], the overall metabolic regulatory roles of SERPINA3C in the pathogenesis of obesity and related metabolic disorders is poorly understood.

Here, we found that SERPINA3C was mainly expressed in WAT, and its protein level was down-regulated upon HFD-induced obesity. Loss of SERPINA3C led to more severe diet-induced obesity (DIO) and insulin resistance, with higher level of inflammation and cell death in adipose tissue. Consistently, AAV8-mediated overexpression of SERPINA3C in inguinal adipose tissue alleviated DIO and improved glucose tolerance and insulin sensitivity in HFD-fed mice, with lower level of inflammation and cell death in adipose tissue. Mechanistically, SERPINA3C, acting as a serine protease inhibitor, inhibited Cathepsin G activity, blocking cathepsin G-mediated turnover of α5 Integrin and β1 Integrin proteins in adipocytes. The α5 Integrin/β1 Integrin signaling was responsible for AKT activity, which controlled JNK activity to inhibit inflammation in adipocytes. Our study demonstrated that SERPINA3C, a WAT-enriched secreted factor, plays a protective role against HFD-induced obesity and insulin resistance in mice. A previously unknown adipose tissue SERPINA3C/Cathepsin G/Integrin/AKT pathway is illustrated in our work, which provides new insights into adipokine-mediated prevention and treatment of obesity and insulin resistance.

2. MATERIAL AND METHODS

2.1. Animals

Mice were fed a chow diet or high-fat diet (HFD) as indicated. Chow-fed mice were housed with 5—6 mice per cage and mice on HFD were housed with 4—5 mice per cage. To produce HFD-induced obese mice, 8-week-old C57BL/6J mice were fed an HFD (60% kcal from fat, D12492; Research Diets) for 16 weeks.

The generation of the SERPINA3C-knockout (KO) mice was commissioned by Shanghai Model Organisms. To generate KO mice, the CRISPR/Cas9 strategy was used to delete exons 2—5 of mouse SERPINA3C by non-homologous recombination. SERPINA3C$^{-/-}$ mice were then obtained by mating the SERPINA3C$^{+/-}$ mice. Genotyping was performed by PCR using the genomic DNA obtained from clipped tails. The primers used for the SERPINA3C gene are shown in Supplementary Table 1. SERPINA3C$^{-/-}$ mice were identified with a single PCR product of 526/588 bp using primers 1 and 2.

For SERPINA3C overexpression, AAV containing the SERPINA3C coding sequence and the control vector were purchased from Shanghai Genechem (Shanghai, China). The 12-week-old mice fed with a 4-week HFD were injected with AAV subcutaneously adjacent to the iWAT.

All the mice were housed at room temperature (25 °C), unless otherwise specified, with a 12-hour light—dark cycle with ad libitum access to food and water. Experiments were performed in age- and sex-matched mice. All studies involving animal experimentation were approved by the Fudan University Shanghai Medical College Animal Care and Use Committee and followed the National Institutes of Health guidelines on the care and use of animals.

2.2. Cell culture and induction of differentiation

The 3T3-L1 preadipocytes were differentiated into mature adipocytes as in our previous studies [21], at 2 days post—confluence (designated day 0), 3T3-L1 were subjected to adipogenic differentiation. Adipocytes' phenotype appeared on day 3 and reached maximum by day 8 post-adipogenic induction. Adipocyte treatments were conducted on day 8.

2.3. Mature adipocytes and stromal vascular fraction (SVF) isolation

Adipose tissues were minced and digested with 0.075% collagenase (C2139, collagenase VIII; Sigma—Aldrich, St. Louis, MO, USA) at 37 °C for 40 min. Digested tissues were strained using a 100 μm mesh filter and centrifuged at 1,600 rpm for 8 min. Adipocytes were then transferred to a new tube, washed with phosphate-buffered saline (PBS), and centrifuged at 1,600 rpm for 8 min for collection.

2.4. Generation of adeno-associated virus (AAV)

For SERPINA3C overexpression in the iWAT, AAV containing the SERPINA3C coding sequence and the control were purchased from Shanghai Genechem.

2.5. Blood metabolite measurements

Blood was collected from the indicated mice after overnight fasting, and serum was prepared for measurement. Serum triglyceride (TG), total cholesterol (TC), high-density lipoprotein (HDL), and low-density lipoprotein (LDL) levels were determined using an automatic biochemical analysis device (Roche, Basel, Switzerland), as previously described [22].

2.6. Animal metabolic measurements

A Comprehensive Lab Animal Monitoring System (CLAMS; Columbus Instruments, Columbus, OH, USA) was used to record O_2 consumption, CO_2 production, energy expenditure, and food intake. Animals were acclimatized in the recording chambers for 72—96 h, and measurements were taken subsequently for 48 h during light and dark cycles, with free access to food and water. Data of O_2 consumption, CO_2 production was corrected by mice lean mass.

2.7. Body composition measurements

We measured the fat and lean mass of live mice using an NMR analyzer (MiniSpec Live Mice Analyzer; Bruker, Fremont, CA, USA) according to the manufacturer's instructions.

2.8. Glucose tolerance test (GTT) and insulin tolerance test (ITT)

For the GTT, mice were injected intraperitoneally with D-glucose (2 mg/g body weight) after fasting for 16 h (from 5 p.m. to 9 a.m.), and blood glucose obtained from tail bleeds was monitored at 15, 30, 60, 90, and 120 min after administration using a glucometer monitor (Johnson & Johnson, Santa Clara, CA, USA). For the ITT, mice were injected intraperitoneally with recombinant human insulin (Novo Nordisk, Fremont, CA, USA) (0.75 IU/kg body weight) after fasting for 4 h (from 8 a.m. to 12 p.m.), and blood glucose levels were monitored at 15, 30, 60, 90, and 120 min after insulin administration.

2.9. In vivo insulin signaling studies

The HFD-fed mice were fasted overnight (12—16 h) and subsequently were injected i.p. with recombinant human insulin (Novo Nordisk) (1.5 IU/kg body weight), and after 15 min, mice were euthanized, and inguinal white adipose tissue (iWAT), epididymal white adipose tissue (eWAT), brown adipose tissue (BAT), liver, and muscle were excised and snapped frozen in liquid nitrogen. Western blot assays were conducted to measure the levels of AKT signaling proteins.

2.10. The 2-deoxyglucose (2-DG) uptake assay

Freshly isolated iWAT, eWAT, BAT, liver, and muscle were excised, cut into pieces and incubated in Krebs—Ringer buffer containing 11.1 mmol/L glucose for 1 h. After the initial incubation period, the tissues were pretreated with or without insulin for 0.5 h, followed by incubation with 200 mmol/L 2-(N-(7-nitrobenz-2-oxa-1,3-diazol-4-yl) amino)-2-deoxyglucose (2-NBDG; Invitrogen, Carlsbad, CA, USA) for 2 h in the absence or presence of insulin. Cells were incubated in Krebs—Ringer buffer and treated in the same way as the experiments conducted using tissues. After 2-DG incubation, the tissues and cells were rinsed and lysed. Fluorescence was measured using an Envision fluorescence microplate reader (Envision, San Jose, CA, USA) and normalized to the total protein concentration.

2.11. Cathepsin G Activity Assay

Cells - The cultured medium from 3T3-L1 cells was collected from cells treated with tumor necrosis factor (TNFα, 20 ng/mL) and/or recombinant SERPINA3C protein. Cathepsin G activity was measured using a Colorimetric Cathepsin G Activity Assay kit (Abcam, Cambridge, UK) according to the manufacturer's protocol.

Mice - Fresh tissues were collected after overnight fasting of the mice. Tissues were lysed in cold PBS and centrifuged at 12000 rpm for 10 min to collect supernatant. Cathepsin G activity was measured using a Colorimetric Cathepsin G Activity Assay kit (Abcam) according to the manufacturer's protocol.

2.12. Caspase-3 Activity Assay

2.12.1. Cells

The cultured medium from 3T3-L1 cells was collected from cells treated with tumor necrosis factor (TNFα, 20 ng/mL) or Cathepsin G recombinant protein (100 ng/mL) and/or recombinant SERPINA3C protein. Caspase-3 activity was measured using a Caspase 3 Activity Assay Kit (Beyotime Biotechnology) according to the manufacturer's protocol.

2.12.2. Mice

Fresh tissues were collected after overnight fasting of the mice. The tissues were lysed and centrifuged at 16000 g for 15 min to collect supernatant. Caspase-3 activity was measured using a Caspase 3 Activity Assay Kit (Beyotime Biotechnology) according to the manufacturer's protocol.

2.13. Histochemistry and immunohistochemistry (IHC)

For hematoxylin-eosin (H&E) staining and IHC staining, tissues were immediately fixed with 3.7% paraformaldehyde at 4 °C overnight, then the formaldehyde-fixed tissues were embedded in paraffin, sectioned, and stained with H&E, or with the F4/80 antibody (ab6640; Abcam; 1:100) following standard procedures, as described previously [23—25].

2.14. Oxygen consumption rate

Freshly isolated iWAT and eWAT (approximately 40—50 mg) or BAT depots (approximately 20 mg) were minced in 1 mL phosphate-buffered saline supplemented with 25 mM glucose, 1 mM pyruvate, and 2% bovine serum albumin. Cultured adipocytes (Day 8) were trypsinized and collected by centrifugation. Cell pellets were resuspended in the abovementioned buffer. Oxygen consumption was measured with a Clark electrode (Oxygraph + system; Hansatech, Pentney, UK) and data were normalized to total tissue weight or total protein contents.

2.15. Measurement of mitochondrial membrane potential

The fluorescent, lipophilic, and cationic probe JC-1 measured the mitochondrial membrane potential ($\Delta\Psi m$) of 3T3-L1 adipocytes according to the manufacturer's directions. Briefly, after the indicated treatments, the cells were incubated with the JC-1 staining solution (2 μmol/L) for 45 min at 37 °C. The cells were then rinsed twice with Hank's balanced salt solution (HBSS) buffer, and the fluorescence intensity of the mitochondrial JC-1 monomers (λex 514 nm and λem 529 nm) and aggregates (λex 585 nm and λem 590 nm) were detected using a Leica confocal microscope (TCS SP8; Leica, Wetzlar, Germany) or fluorescence microscope.

2.16. Flow cytometry analysis

Cells were incubated in a 10% calf serum/PBS block for 30 min at room temperature and stained with the indicated antibodies (Abs) for 40 min on ice, then incubated with Alexa Fluor® 488 secondary antibody for 30 min at room temperature. Abs for flow cytometry are listed in Supplemental Table S3. The cells were analyzed using a FACS Canto II Flow Cytometer (BD Biosciences, San Jose, CA, USA) using FlowJo 10.6 software (Tree Star).

2.17. Real-time quantitative PCR

The mRNA was extracted with TRIzol reagent (Thermo Fisher Scientific, Waltham, MA, USA). For mouse and cell experiments, 1—2 μg of mRNA was amplified with the Thermo Fisher Scientific Maxima H Minus First Strand cDNA Synthesis Kit with dsDNase (Cat. K1682; Thermo Fisher Scientific). Quantitative PCR (qPCR) used a Power SYBR green PCR master mix (Q711-02; Vazyme, Nanjing, China) and a ViiA TM 7 instrument (Applied Biosystems, Foster City, CA, USA), with 36B4 rRNA as an endogenous control. The qPCR primers were designed to span exon—exon sequences to generate a product of 100—200 bp, and the sequences were derived either from the validated PrimerBank (http://pga.mgh.harvard.edu/primerbank) or from published literatures. The sequences of primers are listed in Supplementary Table 2. The mRNA levels of each gene were calculated with the 2ΔddCt method and normalized for the expression of mRNA of the housekeeping gene (as indicated in the figure legends).

2.18. Western blotting

The cells and mouse tissues were lysed with a buffer containing 2% SDS, 10 mM dithiothreitol, 50 mM Tris—HCl (pH 6.8), 10% glycerol, and 0.002% Bromophenol Blue. Soluble lysates were collected by centrifugation at 12,000 rpm for 10 min at 4 °C. The total protein concentration was determined using a bicinchoninic acid assay (Thermo Fisher Scientific). Equal amounts of protein were separated by SDS-PAGE. Proteins were transferred to a PVDF membrane with wet transfer for 90 min at constant 350 mA using the Trans-Blot Turbo transfer system from Bio-Rad (Hercules, CA, USA). Membranes were blocked with 5% milk for 60 min and incubated overnight with the primary antibody in 2% fatty acid-free bovine serum albumin (BSA). Washes were conducted using 1% TTBS (Tris-Tween buffer saline) buffer and secondary antibody was used at 1:8,000 or 1:10,000 for 40 min at room temperature. Antibodies used in this study are listed in

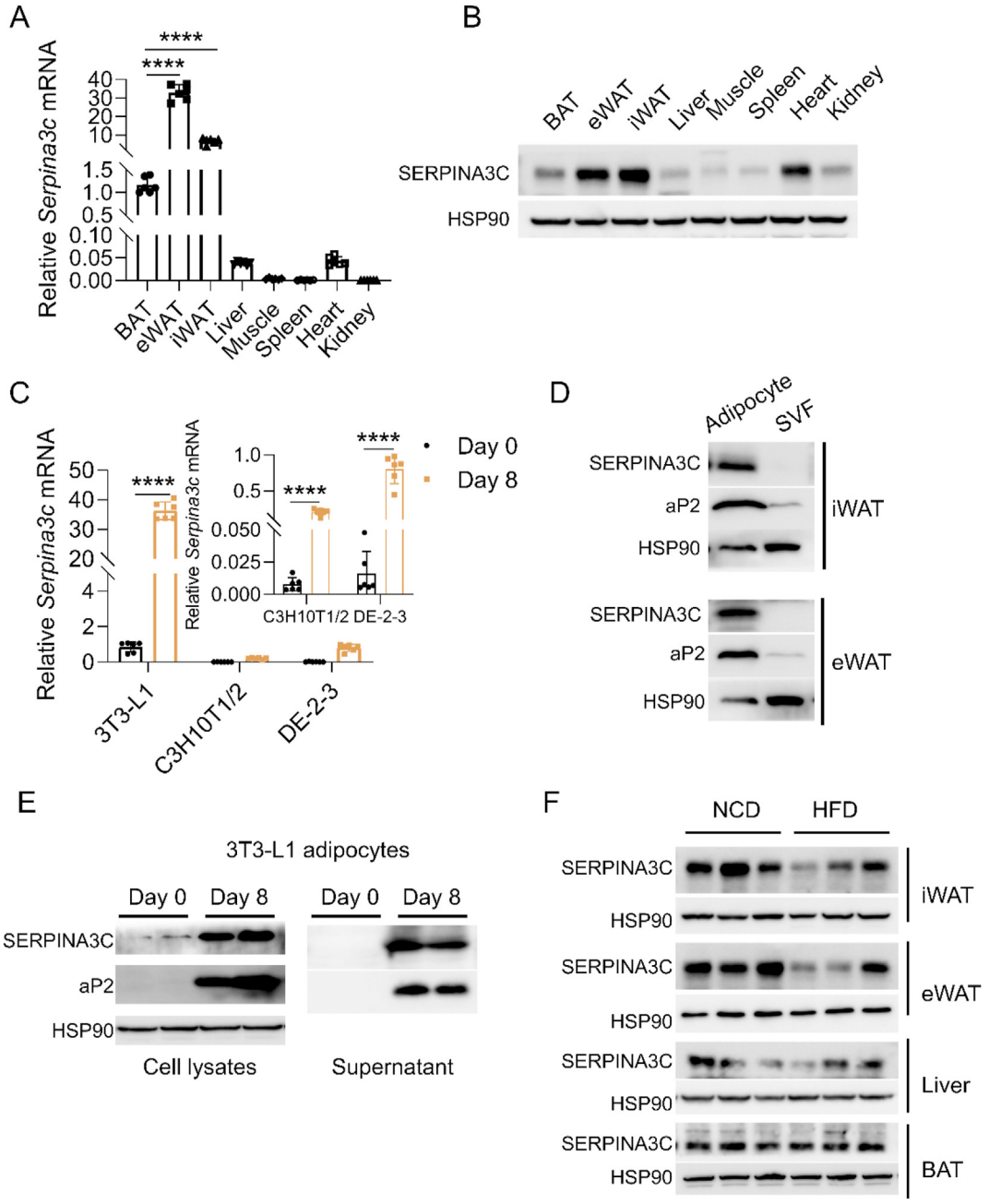

Figure 1: SERPINA3C is a secreted factor enriched in adipocytes and is downregulated in white adipose tissue (WAT) of mice after high-fat diet (HFD) feeding. *A*: The NCD-fed 16-week-old C57BL/6J male mice were sacrificed for analyses. qPCR analysis of SERPINA3C mRNA expression in multiple tissues of the mice was shown. *B*: SERPINA3C protein level in multiple tissues of the mice in (*A*). *C*: qPCR analysis of SERPINA3C mRNA expression before (*Day 0*) and after (*Day 8*) 3T3-L1, C3H10T1/2, DE-2-3 cell differentiation. *D*: SERPINA3C protein level in adipocyte and SVF from iWAT (*above*) and eWAT (*below*) of 12-week-old NCD-fed male mice. *E*: SERPINA3C protein level before (*Day 0*) and after (*Day 8*) 3T3-L1 cell differentiation. *Left,* cell lysates; *right,* supernatant. *F*: 8-week-old male C57BL/6J mice were fed with NCD or HFD for an additional 16 weeks; Western blot analysis of SERPINA3C protein expression in adipose tissue (iWAT, eWAT and BAT) and liver of the mice was shown. $n = 3$. For statistical analyses, one-way analysis of variance and Bonferroni's post hoc tests were performed in (*A*), unpaired two-tailed Student's t tests were performed in (*C*). All values are represented as means with error bars representing S.D. ****, $p < 0.0001$. $n = 6$ for each group unless otherwise mentioned.

Supplementary Table 3. In all blots presented in the manuscript, loading controls were run on the same blot as the protein blots.

2.19. Statistical analysis

All values in graphs are presented as the mean ± SD. Comparisons between groups were made using unpaired two-tailed Student's t-tests. For comparison of three or more independent groups with only one variable, one-way analyses of variance plus Bonferroni's post hoc tests were conducted. For comparison of two or more independent groups with two variables, two-way analysis of variance plus Bonferroni's post hoc tests were conducted. GraphPad Prism 8.0 software (GraphPad, San Diego, CA, USA) was used for all statistical analyses. The statistical analyses were also indicated in the legends of each figure, with $p < 0.05$ being considered statistically significant. All

experiments were repeated a minimum of three times, and representative data are shown.

3. RESULTS

3.1. SERPINA3C is a secreted factor enriched in adipocytes and its expression in white adipose tissue (WAT) is down-regulated upon diet-induced obesity (DIO) in mice

Adipokines play important roles in energy homeostasis. To identify new adipokines, we queried a previously published mouse secretome database [26] for novel secreted factors preferentially expressing in adipose tissue, which included SERPINA3C. SERPINA3C exhibited a highly restricted pattern of expression in adipose tissue and had higher expression in inguinal white adipose tissue (iWAT) and epididymal white adipose tissue (eWAT) than in brown adipose tissue (BAT) (Figure 1A,B). By analyzing the 3T3-L1 cells (a white adipocyte model), C3H10T1/2 cells (a beige-like adipocyte model), and DE-2-3 cells (a brown adipocyte model), SERPINA3C expression was enriched in mature white adipocytes, with very low expression in preadipocytes (Figure 1C). Moreover, western blot analysis of the isolated cell fractions from mice adipose tissues demonstrated that SERPINA3C protein was mainly expressed in mature adipocytes, while negligible SERPINA3C expression was detected in the stromal vascular fractions (SVFs) (Figure 1D). To ensure that SERPINA3C protein was a bona fide secreted factor, cell culture media from pre-adipocytes (Day 0) and mature adipocytes (Day 8) were collected. Western blotting indicated that the SERPINA3C protein level was highly increased in differentiated adipocytes (Figure 1E, *left*). Consistently, cultured media from mature adipocytes also contained higher levels of SERPINA3C protein, indicating that SERPINA3C was a bona fide secreted factor of adipocytes (Figure 1E, *right*). The enriched expression of SERPINA3C in white adipose tissue (WAT) and in mature white adipocytes prompted us to investigate the potential function of SERPINA3C in adipose tissue metabolism.

To determine the potential role of SERPINA3C in metabolic disorders during obesity, we examined the expression of SERPINA3C in mice fed a high-fat diet (HFD). The expression of the SERPINA3C transcript was slightly induced only in iWAT after HFD feeding for 16 weeks (Supplementary Figure 1A), while the SERPINA3C protein level was significantly decreased both in iWAT and eWAT (Figure 1F and Supplementary Figure 1B). The fact that the mRNA level of SERPINA3C in mouse adipose tissues remained unchanged or was slightly increased after HFD feeding suggests some translational regulations or post-translational modifications to impair the expression or stability of SERPINA3C protein under HFD feeding condition. Thus, our results demonstrated that SERPINA3C was an adipocyte-derived secreted factor, and its protein level in adipose tissue was down-regulated during obesity, which suggested that dysregulated SERPINA3C expression could play roles in obesity and related metabolic disorders.

3.2. SERPINA3C ablation exacerbates diet-induced obesity (DIO) and metabolic disorders in mice

To assess the function of SERPINA3C in metabolic homeostasis, we generated global SERPINA3C knockout (KO) mice (Supplementary Figure 2A). Successful deletion of SERPINA3C mRNA (Supplementary Figure 2B) and protein (Supplementary Figure 2C) was detected. Moreover, secreted SERPINA3C protein in the culture medium of the adipose tissues from SERPINA3C—KO mice was not detectable (Supplementary Figure 2D), which further confirmed that SERPINA3C was a secreted factor from adipocytes.

The SERPINA3C—KO mice did not exhibit overt abnormalities and were indistinguishable from the control wild type (WT) mice under normal chow diet feeding. However, after 16 weeks of HFD feeding, diet-induced body weight gain (Figure 2A,B) and fat mass amount (Figure 2C—E) in the SERPINA3C—KO mice were more prominent than those in WT mice. Consistent with more severe adiposity under HFD-fed conditions, SERPINA3C—KO mice had higher serum triglyceride (TG) levels than control WT mice (Figure 2F). However, SERPINA3C—KO mice and their WT control littermates consumed similar amounts of food (Supplementary Figure 2E). An indirect calorimetry study demonstrated that SERPINA3C—KO mice had lower oxygen consumption and lower carbon dioxide production (Figure 2G,H, and Supplementary Figs. 3A and B). Consistently, lower oxygen consumption rates (OCRs) in the iWAT, eWAT, BAT, and livers of SERPINA3C—KO mice than those in WT mice were also observed (Supplementary Figure 3C).

Obesity is closely related to glucose intolerance and insulin resistance [27]. Notably, HFD-fed SERPINA3C—KO mice exhibited more severe glucose intolerance and insulin resistance than control mice, though no obvious change in serum insulin levels (Figure 2I—M). These observations demonstrated that global knockout of SERPINA3C exacerbated diet-induced obesity and disrupted glucose homeostasis in mice.

3.3. HFD-fed SERPINA3C—KO mice exhibit aggravated inflammation, apoptosis and insulin resistance in adipose tissue

Mounting evidence shows that inflammation in metabolic tissues is an important mediator in the development of glucose intolerance and insulin resistance [28]. The role of SERPINA3C deficiency in adipose tissue inflammation was therefore determined in HFD-fed mice. Histological staining revealed larger size of lipid droplets in the iWAT and eWAT of SERPINA3C—KO mice following HFD feeding (Figure 3A—D), demonstrating hypertrophy of adipose tissue which is usually associated with adipose tissue dysfunction. Meanwhile, quantitative real-time PCR (qPCR) analyses indicated that mRNA expression of inflammatory genes like PYD domains-containing protein 3 *(Nlrp3)*, tumor necrosis factor α (*Tnf*α), interleukin 1β *(Il-1*β*)*, *Il-6*, *Il-18*, and monocyte chemoattractant protein 1 *(Mcp1)* in iWAT and eWAT were significantly increased in KO mice, when compared with control mice (Figure 3E,F). Increased inflammation can lead to cell death, which will exacerbate metabolic disorders [29]. Indeed, SERPINA3C—KO promoted cell apoptosis in adipose tissue, as caspase-3 activity was markedly increased in iWAT and eWAT in SERPINA3C—KO mice, when compared with control mice (Figure 3G). SERPINA3C deficiency slightly affected inflammatory gene expressions in other metabolic tissues like BAT, liver, and muscle (Supplementary Figs. 4A—C). To identify the molecular pathways leading to increased inflammation in SERPINA3C—KO mice, we performed western blot analysis of adipose tissues of SERPINA3C—KO and WT littermates. Previous reports showed that the c-Jun NH_2-terminal kinase isoform, JNK, was a critical regulator of inflammation, which has been implicated in the mechanism of obesity-induced insulin resistance. HFD feeding caused activation of the JNK signaling pathway, insulin resistance, and obesity in mice [30]. In addition to pronounced inflammation in KO mice, SERPINA3C—KO led to enhanced activation of JNK in iWAT and eWAT (Figure 3H,I, respectively). Compared with the samples of WT groups, mild trends of increased JNK phosphorylation level, but without significant differences, were observed in BAT, liver and muscle of SERPINA3C—KO mice (Supplementary Figs. 4D—I). We also examined the role of SERPINA3C in regulating the activity of AKT, because AKT is phosphorylated in response to a variety of signals and is an important inhibitory signaling factor of inflammation [31]. Phosphorylation of AKT

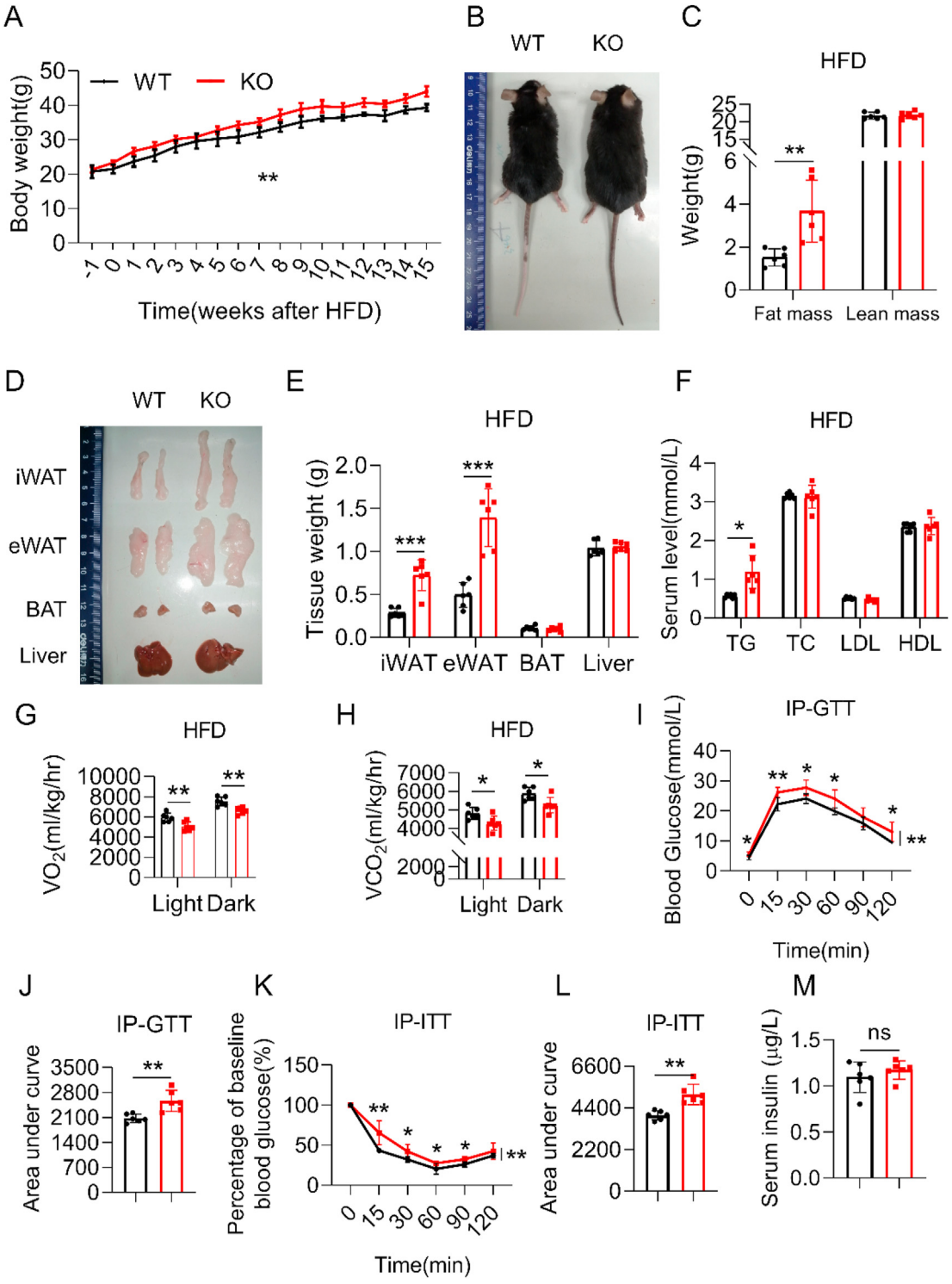

Figure 2: SERPINA3C ablation led to exacerbated diet-induced obesity (DIO) and metabolic disorders in mice. The 8-week-old WT and SERPINA3C-KO mice were fed a HFD for 16 weeks before being sacrificed for analysis. *A*: Body weight (BW) of these WT and KO mice. *B*: Representative pictures of the mice. *C*: Body composition of the mice measured by nuclear magnetic resonance. *D*: Representative images of adipose tissues and livers of the mice. *E*: Weights of adipose tissues and liver of the mice. *F*: Serum TG, TC, LDL, HDL levels of the mice after overnight fasting. *G*: The average values of the whole-body oxygen consumption rate (VO_2) were measured by metabolic cages for the mice. *H*: The average values of the whole-body CO_2 generation (VCO_2) were measured by metabolic cages for the mice. *I*: Glucose concentrations during an i.p. glucose tolerance test (GTT) in mice after 10 weeks of HFD feeding. *J*: Area under the curve analysis of (*I*). *K*: Glucose concentrations during an insulin tolerance test (ITT) in mice after 11 weeks of HFD feeding. *L*: Area under the curve analysis of (*K*). *M*: Serum insulin level of the mice at basal condition of (*K*). For statistical analyses, two-way analysis of variance and Bonferroni's post hoc tests were performed in (*A*), (*I*), and (*K*). Unpaired two-tailed Student's t tests were performed in (*C*), (*E*), (*F*), (*G*), (*H*), (*J*), (*L*) and (*M*). For statistical analyses in (*A*), (*C*), (*E*)–(*L*), data were compared between the WT and KO mice. All values are represented as means with error bars representing S.D. *, $p < 0.05$; **, $p < 0.01$; ***, $p < 0.001$. $n = 6$ for each group.

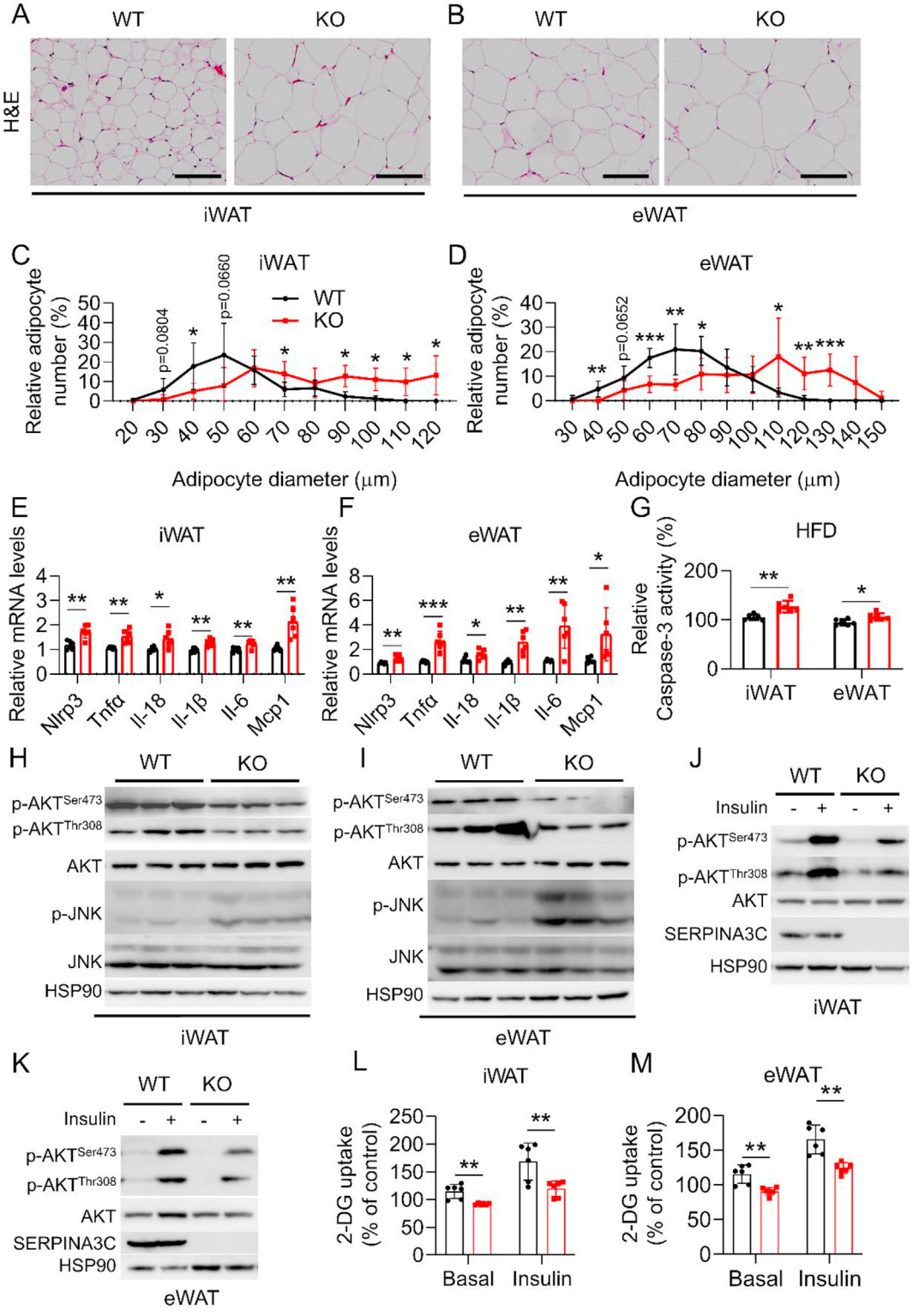

Figure 3: HFD-fed SERPINA3C knockout (KO) mice exhibit aggravated inflammation, apoptosis and insulin resistance in adipose tissue. Mice were treated as indicated in Figure 2. *A* and *B*: H&E staining of iWAT (*A*) and eWAT (*B*), respectively. *Scale bar*, 100 μm. *C* and *D*: Quantitative analyses of adipocyte size distribution of (*A*) and (*B*). *E* and *F*: mRNA levels of the indicated genes were determined by qPCR in iWAT (*E*) and eWAT (*F*), respectively. *G*: Caspase-3 activity was determined in iWAT and eWAT. *H* and *I*: Western blot analysis of the protein levels in iWAT and eWAT by using the indicated antibodies. HSP90 serves as an internal control. *J* and *K*: Western blot for detecting phosphorylated AKT in iWAT and eWAT. Mice were sacrificed 15 min after insulin injection (i.p.). $n = 3$. *L* and *M*: 2-DG uptake was determined in iWAT and eWAT. For statistical analyses, unpaired two-tailed Student's t tests between the WT and KO mice were performed in (*E*)–(*G*), (*L*) and (*M*). All values are represented as means with error bars representing S.D. *, $p < 0.05$; **, $p < 0.01$; ***, $p < 0.001$. $n = 6$ for each group unless otherwise mentioned.

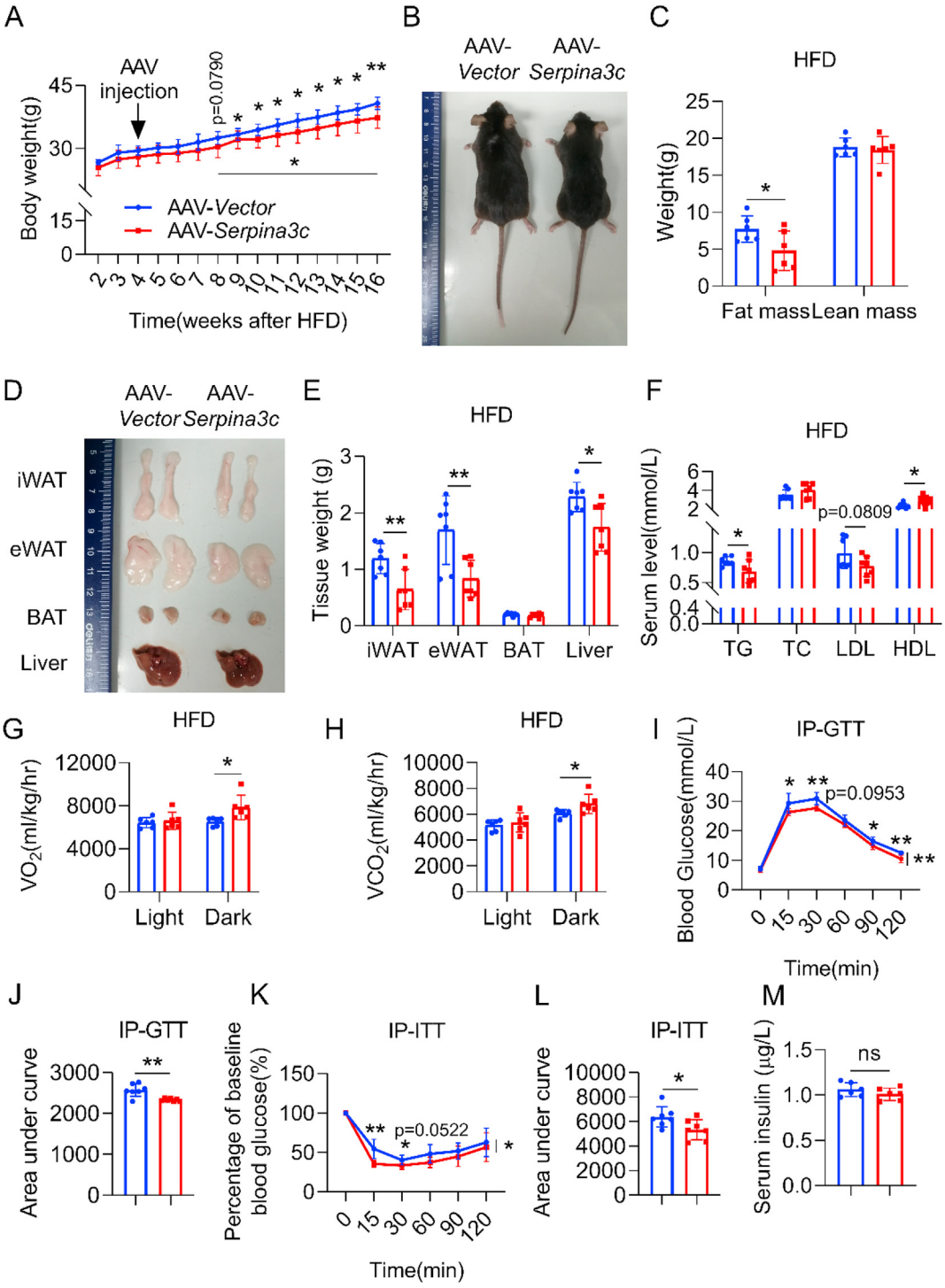

Figure 4: Overexpression of SERPINA3C in inguinal white adipose tissue (iWAT) protects mice against DIO and metabolic disorders. 8-week-old C57BL/6J male mice with 4-week HFD feeding were injected with AAV in iWAT locally. HFD feeding was continued until mice were 24-week-old before mice were sacrificed for analyses. *A*: BW of the mice during 16-week HFD feeding. *B*: Representative picture of the mice after 16-week HFD feeding. *C*: Body composition in the mice was measured by nuclear magnetic resonance. $n = 6$. *D*: Representative images of adipose tissues and liver from the mice. *E*: Weights of adipose tissues and liver from the mice. *F*: Serum TG, TC, LDL, HDL levels of the mice after overnight fasting. *G*: The average values of the whole-body oxygen consumption rate (VO_2) were measured by metabolic cages for the mice. $n = 6$. *H*: The average values of the whole-body CO_2 generation (VCO_2) were measured by metabolic cages for the mice. $n = 6$. *I*: Glucose concentrations during an i.p. glucose tolerance test (GTT) after mice were injected with AAV for 3 weeks. *J*: Area under the curve analysis of (*I*). *K*: Glucose concentrations during an insulin tolerance test (ITT) after mice were injected with AAV for 4 weeks. *L*: Area under the curve analysis of (*K*). *M*: Serum insulin level of the mice at basal condition of (*K*). For statistical analyses, two-way analysis of variance and Bonferroni's post hoc tests were performed in (*A*), (*I*), and (*K*). Unpaired two-tailed Student's t tests were performed in (*C*), (*E*), (*F*), (*G*), (*H*), (*J*), (*L*) and (*M*). For statistical analyses in (*A*), (*C*), (*E*)–(*L*), data were compared between the AAV-Vector and AAV-SERPINA3C mice. All values are represented as means with error bars representing S.D. *, $p < 0.05$; **, $p < 0.01$. $n = 7$ for each group unless otherwise mentioned.

at Ser473 and Thr308 were both attenuated in the iWAT and eWAT of SERPINA3C—KO mice (Figure 3H,I, respectively). These results suggest that damaged AKT signaling and enhanced JNK activity may contribute to the aggravated adipose inflammation in SERPINA3C—KO mice during DIO.

Muscle, liver, and fat are important target tissues of insulin. To study whether the insulin sensitivity of the above organs was affected by SERPINA3C—KO, HFD-fed mice were intraperitoneally injected with saline or insulin, and the above tissues were collected for analyses. Basal and insulin-induced AKT phosphorylation was attenuated in iWAT and eWAT of SERPINA3C—KO mice (Figure 3J,K, and Supplementary Figs. 4J and K). A lower rate of 2-deoxyglucose (2-DG) uptake in the WAT of SERPINA3C—KO mice than those in WT mice was also observed (Figure 3L,M). Similar experiments were also performed in BAT, liver, and muscle, which showed slight changes, but with similar trends (Supplementary Figure 4L-Q), indicating that SERPINA3C-ablated mice exhibited aggravated inflammation and insulin resistance in metabolic organs, especially in WAT. In summary, these results demonstrate that SERPINA3C deletion exacerbated diet-induced inflammation and insulin insensitivity in metabolic tissues, especially adipose tissue in mice.

3.4. Overexpression of SERPINA3C in iWAT protects mice against DIO and metabolic disorders

To explore whether overexpression of SERPINA3C in adipose tissue could improve metabolic health in DIO mice, mice were subjected to subcutaneous injection in the iWAT with adeno-associated virus (AAV) containing a control vector or a vector encoding the SERPINA3C gene, after 4 weeks of HFD feeding (Supplementary Figure 5A). AAV-mediated SERPINA3C overexpression was confirmed, which showed that SERPINA3C was overexpressed efficiently in iWAT (Supplementary Figs. 5B and C). The body weights of the AAV-Vector- and AAV-SERPINA3C-treated mice started to diverge after 8 weeks of HFD feeding (Figure 4A), but with a similar food intake (Supplementary Figure 5D); while the AAV-SERPINA3C-treated mice gained less weight (Figure 4A,B). This was associated with less total fat mass, i.e. less mass in iWAT and eWAT of the AAV-SERPINA3C-treated mice (Figure 4C—E). Accordingly, AAV-SERPINA3C treatment slightly decreased serum TG and low-density lipoprotein (LDL) levels, and mildly increased high-density lipoprotein (HDL) levels (Figure 4F). The reduced adiposity in the AAV-SERPINA3C-treated mice might be related to increased energy expenditure, because the AAV-SERPINA3C-treated mice exhibited higher oxygen consumption and higher carbon dioxide production (Figure 4G,H, and Supplementary Figs. 6A and B). Consistently, mice with SERPINA3C overexpression in iWAT showed a significantly increased OCR in iWAT, eWAT, BAT, and the liver (Supplementary Figure 6C).

Furthermore, the injection of AAV-SERPINA3C in iWAT also resulted in improvement in glucose metabolism, as shown by ameliorative glucose intolerance and increased insulin sensitivity after 3 weeks of AAV injections with insignificant difference in serum insulin level (Figure 4I—M), at a time point when the weight difference was not significantly different between the two groups. Together, these results demonstrated that WAT-derived SERPINA3C played an important role in mitigating DIO and metabolic disorders.

3.5. HFD-fed mice with adipose tissue specific overexpression of SERPINA3C are protected from HFD-induced inflammation, apoptosis and insulin resistance in adipose tissue

To evaluate whether improved metabolism by SERPINA3C overexpression in iWAT was associated with decreased inflammation, histological studies on adipose tissue were performed and the results revealed that AAV- SERPINA3C-treated mice exhibited less hypertrophy of adipose tissue in WAT compared to the AAV-Vector-treated mice (Figure 5A—D). Expression of proinflammatory markers were determined in iWAT and eWAT of AAV-Vector and AAV-SERPINA3C-treated DIO mice. The qPCR analysis demonstrated that the gene expressions of *Nlrp3*, *Tnfα*, *Il-18*, *Il-1β*, *Il-6*, and *Mcp1* were significantly lower in the AAV-SERPINA3C mice than in control mice (Figure 5E,F), with iWAT showing a more obvious difference. In consistence with less severe inflammation, the level of cell apoptosis was lower in iWAT of AAV-SERPINA3C-treated mice than in the control mice, with weaker downtrend in eWAT, as indicated by caspase-3 activity determination (Figure 5G). The expression of inflammatory genes showed slight changes but with similar trends in other metabolic tissues like BAT, liver, and muscle (Supplementary Figs. 7A—C). Consistently, western blot analyses revealed that AKT phosphorylation was more pronounced, while JNK activity was downregulated, in iWAT and eWAT of SERPINA3C-overexpressed mice (Figure 5H,I), when compared to the AAV-Vector-treated control group. The basal and insulin-stimulated phosphorylation of AKT (Ser 473 and Thr308) were higher in the iWAT and eWAT of AAV-SERPINA3C-treated mice than those in the control group (Figure 5J,K, and Supplementary Figs. 7D and E). Consistently, the ability of 2-DG uptake was higher in iWAT and eWAT of AAV-SERPINA3C mice (Figure 5L,M). Modest changes with similar trends were also observed in the BAT, liver, and muscle (Supplementary Figs. 7F—K).

Taken together, our data suggest the anti-inflammation potential of SERPINA3C which may contribute to its protective effects against obesity and metabolic disorders. Studies have established a consensus that inflammatory mediators impaired mitochondrial metabolism, and that defective mitochondrial function led to decreased energy expenditure, which contributes to the initiation and progression of obesity [32—34]. Based on our data, positive correlation between SERPINA3C expression level and energy expenditure, and negative correlation between SERPINA3C expression level and obesity were observed. Moreover, investigation of OCR in adipose tissue indicated that SERPINA3C facilitated oxygen consumption (Supplementary Figure 3C; Supplementary Figure 6C). We then determined whether SERPINA3C promoted oxygen consumption by inhibiting inflammation-mediated impairment of mitochondrial function in adipocytes. To test this hypothesis, we first treated adipocytes with TNFα, an important inflammation mediator, which can decrease OCR (Supplementary Figure 8A). In the presence of SERPINA3C recombinant protein, however, TNFα-mediated inhibition of OCR was recovered in adipocytes (Supplementary Figure 8A). This was further confirmed by the presence of reduced JC-1 red aggregates upon TNFα-treatment and restored JC-1 red aggregates in the presence of SERPINA3C (Supplementary Figs. 8B and C). Inflammation and mitochondrial dysfunction would cause cell death. In consistence with the results above, Caspase-3 activity was induced by TNFα and was reverted by SERPINA3C, which indicates that SERPINA3C can inhibit TNFα-induced apoptosis of adipocytes (Supplementary Figure 8D). Together, these results suggest that SERPINA3C improved glucose balance and promoted energy expenditure via inhibiting inflammation and maintaining mitochondrial function in adipocytes during obesity.

3.6. SERPINA3C improves metabolic health at least partially via inhibiting Cathepsin G-mediated inflammation in adipocytes

The above results implied that WAT-derived SERPINA3C protected mice from obesity and glucose imbalance through an autocrine and/or paracrine way. The underlying mechanism for the action of SERPINA3C

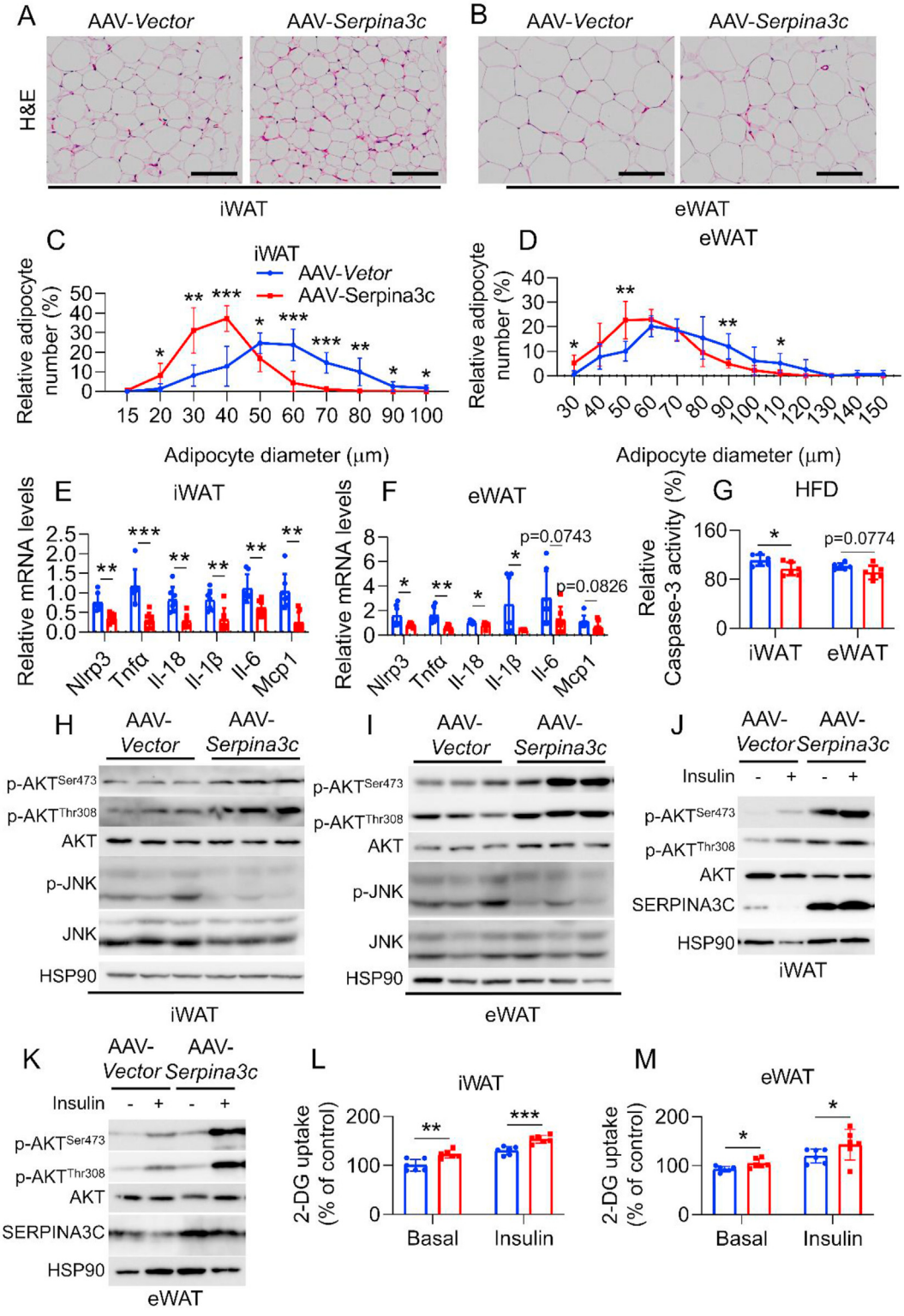

Figure 5: HFD-fed mice with SERPINA3C overexpressing in the iWAT were protected from HFD-induced inflammation, apoptosis and insulin resistance in adipose tissue. Mice were treated as indicated in Figure 4. *A* and *B*: H&E staining of iWAT (*A*) and eWAT (*B*), respectively. *Scale bar*, 100 μm. *C* and *D*: Quantitative analyses of adipocyte size distribution of (*A*) and (*B*). *E* and *F*: mRNA levels of the indicated genes were determined by qPCR in iWAT (*E*) and eWAT (*F*), respectively. *G*: Caspase-3 activity was determined in iWAT and eWAT. *H* and *I*: Western blot analysis of the protein levels in iWAT and eWAT, respectively, by using the indicated antibodies. HSP90 serves as an internal control. *J* and *K*: Western blot for detecting phosphorylated AKT in iWAT and eWAT, respectively. Mice were sacrificed 15 min after insulin injection (i.p.). $n = 3$. *L* and *M*: 2-DG uptake was determined in iWAT and eWAT, respectively. $n = 6$. For statistical analyses, unpaired two-tailed Student's t tests between the AAV-Vector and AAV-SERPINA3C mice were performed in (*E*)—(*G*), (*L*), and (*M*). All values are represented as means with error bars representing S.D. *, $p < 0.05$; **, $p < 0.01$; ***, $p < 0.001$. $n = 7$ for each group unless otherwise mentioned.

was then investigated. It has been reported that human *SERPINA3* was a homologous gene for SERPINA3C and tissue protease Cathepsin G was a target of SERPINA3 [13].

We therefore first determined the activity of Cathepsin G in serum and tissues of lean and DIO mice. Cathepsin G activity was robustly induced in obese mice, when compared to lean mice, both in the serum and WATs, while the activity was not affected in the BAT, liver, and heart (Figure 6A,B). We then determined Cathepsin G activity in SERPINA3C—KO mice, AAV-SERPINA3C mice, and the corresponding control mice. Compared to control mice, Cathepsin G activity was enhanced in SERPINA3C—KO mice, both in serum and in WATs (Figure 6C,D). In contrast, Cathepsin G activity was lower in the serum and WATs of AAV-SERPINA3C mice (Figure 6E,F). However, the mRNA expression of Cathepsin G was not affected much in the experimental groups tested above (Supplementary Figure 9A, B and C).

To confirm the possible role of decreased Cathepsin G activity during the anti-inflammation effects of SERPINA3C, we determined whether Cathepsin G treatment induced inflammation in adipocytes. As indicated, inflammation-related genes were upregulated after treating adipocytes with Cathepsin G, whereas this induction was abolished in the presence of SERPINA3C, suggesting that the decrease of Cathepsin G activity might account for the protective role of SERPINA3C against inflammation in adipocytes (Figure 6G). Phosphorylation of AKT, which could inhibit inflammation, was reduced in Cathepsin G-treated adipocytes, when compared with the control group, but this effect was blunted in the presence of SERPINA3C (Figure 6H,I). Meanwhile, SERPINA3C could promote AKT phosphorylation, which was blocked by Cathepsin G (Figure 6H,I). In consistence with the notion that inflammation could impair insulin resistance, Cathepsin G compromised the 2-DG uptake of adipocytes (Figure 6J). However, SERPINA3C treatment partially restored the Cathepsin G-mediated impairment of 2-DG uptake (Figure 6J). In the meantime, Cathepsin G blunted the role of SERPINA3C in promoting 2-DG uptake of the adipocytes (Figure 6J). Moreover, we observed that SERPINA3C increased oxygen consumption in adipocytes, which was significantly downregulated in the presence of Cathepsin G (Figure 6K). JC-1 staining indicated that Cathepsin G treatment impaired the increase of mitochondrial membrane potential mediated by SERPINA3C (Figure 6L,M), suggesting that SERPINA3C promoted oxygen consumption of adipocytes by suppressing Cathepsin G-mediated impairment of mitochondrial function. Furthermore, SERPINA3C-inhibited apoptosis of adipocytes was also attenuated by Cathepsin G, as indicated by caspase-3 activity determination (Figure 6N). Collectively, these data demonstrated that SERPINA3C preserved metabolic homeostasis in adipose tissue, which occurred at least partially by inhibiting Cathepsin G activity to suppress inflammation in adipocytes.

3.7. SERPINA3C protects against adipose inflammation by inhibiting Cathepsin G-mediated turnover of integrin α5/β1 protein to induce AKT activity

Both our *in vivo* and *in vitro* results indicated positive correlation between SERPINA3C and AKT activity, which led us to postulate that AKT signaling may drive the protective effects of SERPINA3C against inflammation. To address this possibility, we added AKT inhibitor to SERPINA3C-treated adipocytes. The role of SERPINA3C in inhibiting inflammation genes expression was attenuated by the AKT inhibitor (Figure 7A). In addition, inhibition of JNK signaling by SERPINA3C was also blunted when AKT inhibitor was added (Figure 7B,C).

Our *in vitro* studies indicated that the extracellular SERPINA3C-mediated inhibition of Cathepsin G activity could facilitate intracellular AKT signaling, which results in ameliorated inflammation in adipocytes (Figure 6G—N). An important question was how this extracellular SERPINA3C/Cathepsin G axis affects intracellular AKT signaling. A previous study reported that Cathepsin G proteolytically modified integrins on platelets [35]. Integrins are heterodimeric transmembrane receptors that transduce signals through the plasma membrane to activate intracellular signaling. Integrin signaling therefore plays a vital role in "outside-in" signal transmission [36,37]. Integrins are heterodimeric transmembrane receptors composed by α- and β-subunits, which to date have been shown to assemble into 24 distinct integrin types [38]. Among these, β1 Integrin-containing integrins are the largest group of integrins and are thought to be the predominant integrins in adipocytes [38,39]. Moreover, previous studies indicated that β1 Integrin deletion in muscle might lead to insulin resistance [40]. Because adipose SERPINA3C was found to play protective role against insulin resistance in our study, the involvement and mechanism of β1 Integrin in the regulation of adipose tissue metabolism by SERPINA3C was then investigated. β1 Integrin is known to form heterodimers with α5 Integrin to activate AKT signaling [44,46—51]. We examined α5 Integrin and β1 Integrin protein expressions in KO and AAV-SERPINA3C mice. Western blotting showed that SERPINA3C-KO decreased the protein levels of α5 and β1 Integrin in iWAT (Figure 7D), but did not affect their mRNA expression levels (Supplementary Figure 9D). The α6 and αV Integrins and β3 and β5 Integrins, which exhibited relative high expression levels in adipose tissues, were also determined. But their expression was not affected by the deficiency of SERPINA3C (Figure 7D). Accordingly, the protein levels, but not mRNA levels, of α5 and β1 Integrins in iWAT were increased in AAV-SERPINA3C-treated mice, when compared to AAV-Vector-treated mice (Figure 7E and Supplementary Figure 9E). These results suggest the possible involvement of α5/β1 Integrin signaling in the beneficial function of SERPINA3C. Moreover, western blotting revealed that α5 Integrin and β1 Integrin proteins were decreased by Cathepsin G treatment in adipocytes, but this effect was almost completely attenuated in the presence of SERPINA3C (Figure 7F,G). This result was further evidenced by flow cytometry assays, in which Cathepsin G treatment of adipocytes decreased the protein levels of α5 and β1 Integrins on adipocyte plasma membranes, which was rescued by the treatment with SERPINA3C (Figure 7H). Meanwhile, the mRNA levels of α5 and β1 Integrin were unaffected by Cathepsin G and SERPINA3C (Supplementary Figure 9F).

To further characterize the role of Integrin signaling in SERPINA3C-mediated inhibition of inflammation, 3T3-L1 adipocytes were stimulated with a specific α5/β1 Integrin antagonist, ATN-161. Western blot analysis showed that SERPINA3C increased AKT activity and decreased JNK activity under both basal and TNFα-treated conditions. These effects were blunted when α5/β1 Integrin signaling was blocked by ATN-161 (Figure 7I,J). Besides, SERPINA3C inhibited inflammation under basal and TNFα stimulated condition (Figure 7K and Supplementary Figure 10A). However, addition of the antagonist, ATN-161, impaired the anti-inflammatory effect of SERPINA3C (Figure 7K and Supplementary Figure 10A). Inflammation is known to inhibit the insulin sensitivity of adipocytes. As indicated, SERPINA3C enhanced insulin-triggered 2-DG uptake in adipocytes, which was abolished by ATN-161 (Figure 7L). To further confirm the above results, α5 Integrin and β1 Integrin knockdown assays using small interfering RNA (siRNA) were conducted. Downregulation of α5 Integrin and β1 Integrin by siRNAs reproduced the effects of ATN-161 treatment (Supplementary Figs. 10B—D). These results demonstrated that Cathepsin G impaired α5/β1 Integrin signaling in adipocytes to exacerbate adipocyte inflammation and insulin resistance, which was rescued by SERPINA3C. Collectively, our data identified SERPINA3C as an adipokine that

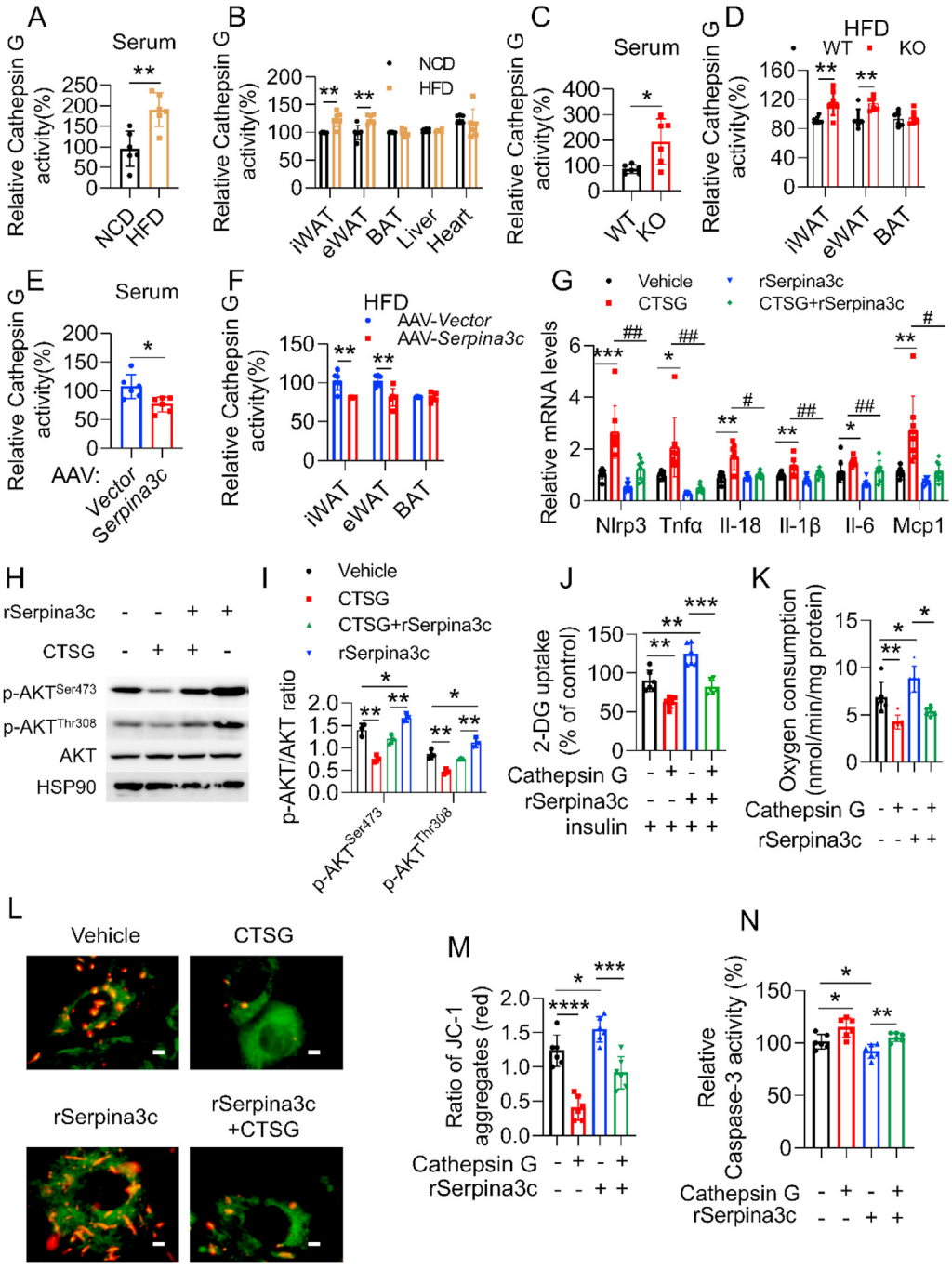

Figure 6: SERPINA3C improves metabolic health at least partially via inhibiting Cathepsin G-mediated inflammation in adipocytes. *A* and *B*: 8-week-old C57BL/6J male mice was fed with NCD or HFD for 16 weeks before being sacrificed. Cathepsin G activity was determined in serum (*A*) and multiple tissues (*B*) of the mice, respectively. *C* and *D*: 8-week-old WT and SERPINA3C−KO male mice was fed with HFD for 16 weeks before being sacrificed. Cathepsin G activity was determined in serum (*C*) and fat tissues (*D*) of the mice, respectively. *E* and *F*: 8-week-old C57BL/6J male mice with 4-week HFD feeding was injected with AAV at iWAT, and then HFD feeding was continued for another 12 weeks before mice were sacrificed. Cathepsin G activity was determined in serum (*E*) and fat tissues (*F*) of the mice, respectively. *G*: 3T3-L1 adipocytes were treated with Cathepsin G and/or SERPINA3C for 12 h, then cells were harvested for analyses. mRNA levels of the indicated genes were determined by qPCR. $n = 8$. *H*: 3T3-L1 adipocytes were treated with Cathepsin G and/or SERPINA3C for 12 h, then cells were harvested. Western blot was used to detect phosphorylated AKT. *I*: Quantification of WB shown in (*H*). Image J was used to calculate band intensities. $n = 3$. *J*: 3T3-L1 adipocytes were pretreated with Cathepsin G and/or SERPINA3C for 12 h, then supplemented with insulin for 10min before harvest. 2-DG uptake assay was used to measure glucose uptake. *K*: OCR is measured by Clark oxygen electrode in Cathepsin G-treated mature 3T3-L1 adipocytes (*Day 8*) with or without SERPINA3C recombinant protein (100 ng/mL) for 12 h. *L*: JC-1 staining of Cathepsin G-treated mature 3T3-L1 adipocytes (*Day 8*) with or without SERPINA3C recombinant protein (100 ng/mL) for 12 h. The subcellular localization of JC-1 monomers (green) and JC-1 aggregates (red) was examined by using a fluorescence microscope. Scale bar: 200 μm. *M*: Quantification of JC-1 aggregates (red) shown in (*L*). *N*: 3T3-L1 adipocytes were treated with Cathepsin G and/or SERPINA3C for 12 h, then cells were harvested for analyses. Caspase-3 activity was determined. For statistical analyses, one-way analysis of variance and Bonferroni's post hoc tests were performed in (*G*), (*I*), (*J*), (*K*), (*M*) and (*N*), unpaired two-tailed Student's t tests were performed in (*A*)—(*F*). All values are represented as means with error bars representing S.D. *, $p < 0.05$; **, $p < 0.01$. #, $p < 0.05$; ##, $p < 0.01$. $n = 6$ for each group unless otherwise mentioned.

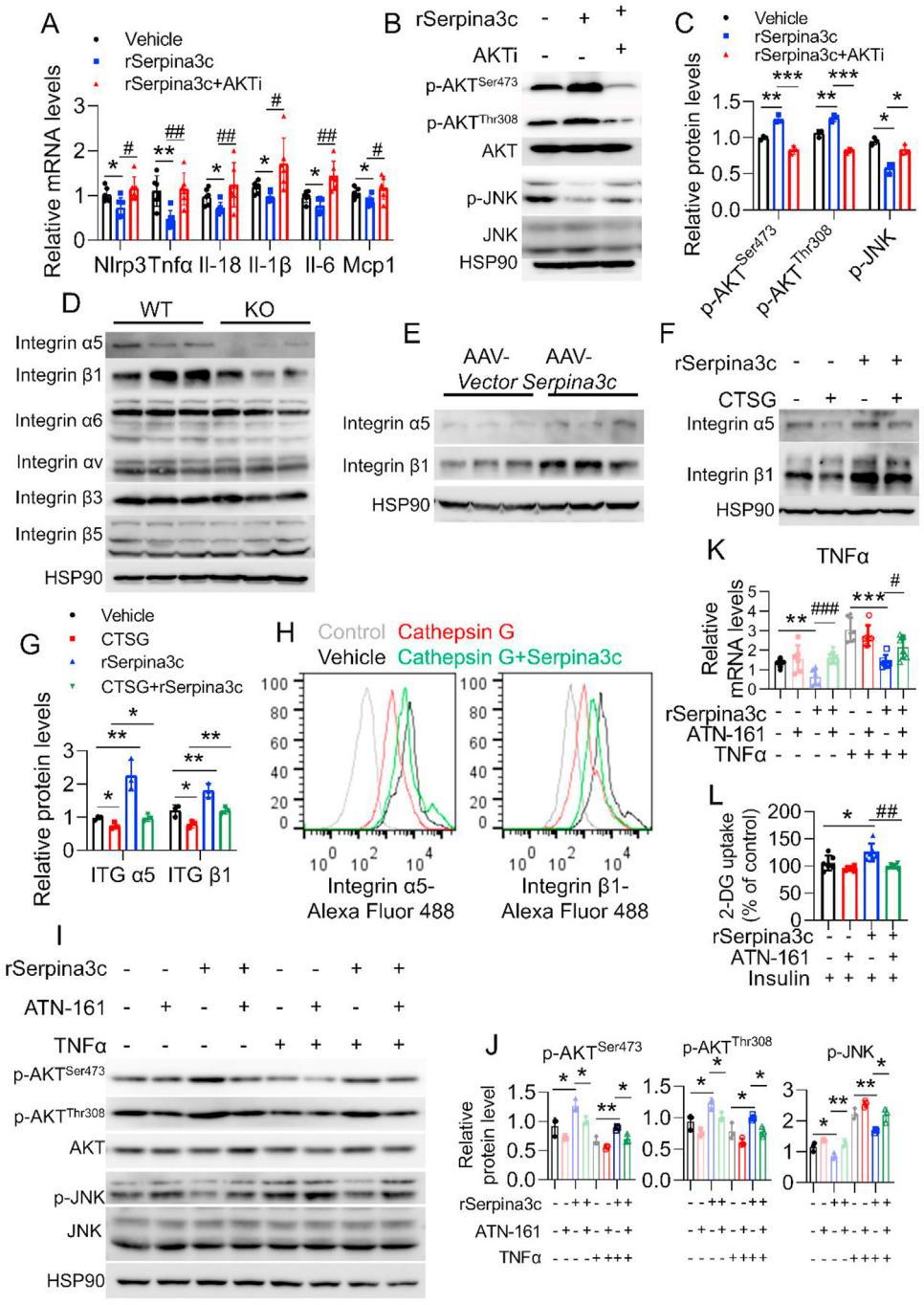

Figure 7: SERPINA3C protects against adipose inflammation by inhibiting Cathepsin G-mediated turnover of Integrin α5/β1 protein to induce AKT activity. *A* and *B*: 3T3-L1 adipocytes were pretreated with TNFα for 12 h. Then SEPRINA3C and AKT inhibitor was added into the cell culture medium as indicated. mRNA levels of the indicated genes were determined by qPCR in (*A*). Western blot analysis of the indicated protein levels was performed in (*B*). *C*: Quantification of WB shown in (*B*). Image J was used to calculate band intensities. $n = 3$. *D*: 8-week-old WT and SERPINA3C—KO male mice were fed with 16-week HFD before being sacrificed. Protein levels of integrin α5, β1, α6, αv, β3, and β5 were determined. $n = 3$. *E*: 8-week-old C57BL/6J male mice with 4-week HFD feeding were injected with AAV at iWAT, and then HFD feeding was continued for another 12 weeks before mice were sacrificed. Protein levels of integrin α5 and integrin β1 were determined. $n = 3$. *F*: Cells were treated with Cathepsin G and/or SERPINA3C for 12 h. Protein levels of integrin α5 and integrin β1 were determined. *G*: Quantification of WB shown in (*F*). Image J was used to calculate band intensities. $n = 3$. *H*: Flow cytometry analysis of the indicated protein levels in Cathepsin G or SERPINA3C treated adipocytes. Cells were treated with Cathepsin G and/or SERPINA3C for 12 h. *I*: 3T3-L1 adipocytes were treated with TNFα and/or SERPINA3C for 12 h, in the presence or absence of 10 μmol ATN-161 (an inhibitor of integrin α5/β1 signaling). Western blot analysis of the indicated protein levels was performed. *J*: Quantification of WB shown in (*I*). Image J was used to calculate band intensities. $n = 3$. *K*: 3T3-L1 adipocytes were treated with TNFα and/or SERPINA3C for 12 h, in the presence or absence of 10 μmol ATN-161. mRNA levels of *TNFα* were determined by qPCR. *L*: SERPINA3C-treated 3T3-L1 adipocytes were stimulated with insulin, ATN-161 was added to block integrin α5/β1 signaling. 3T3-L1 adipocytes were treated with SERPINA3C and/or ATN-161 for 12 h. Then cells were stimulated with or without insulin (100 nmol/L) for 10 min before being harvested. 2-DG uptake assay was performed. For statistical analyses, one-way analysis of variance and Bonferroni's post hoc tests were performed in (*A*), (*C*), (*G*), (*J*), (*K*) and (*L*). All values are represented as means with error bars representing S.D. *, $p < 0.05$; **, $p < 0.01$, ***, $p < 0.001$. #, $p < 0.05$; ##, $p < 0.01$; ###, $p < 0.001$. $n = 6$ for each group unless otherwise mentioned.

controlled inflammation and enhanced insulin sensitivity in adipocytes through the Cathepsin G/α5/β1 Integrin/AKT pathway.

4. DISCUSSION

Accumulating evidence indicates that obesity is associated with chronic low-grade inflammation, which leads to systemic metabolic dysfunction like insulin resistance. Adipose tissue inflammation and its associated cell death has been recognized as important factors in the initiation and progression of metabolic disorders [2]. In the present study, we defined an adipose tissue SERPINA3C/Cathepsin G/Integrin pathway that plays an important role in controlling adipose tissue inflammation and cell death to improve systemic metabolism.

As shown in Figure 1F and Figs. S1A—S1B, western blotting results indicated that high-fat diet (HFD) decreased SERPINA3C protein expression in inguinal white adipose tissue (iWAT) and epididymal white adipose tissue (eWAT), but not Serpina3c mRNA level. Systematic studies quantifying transcripts and proteins at genomic scales revealed the importance of multiple processes beyond transcript abundance that determine the expression level of a protein, including the regulation of protein stability. Mounting evidence indicates that HFD-induced stress-signals can affect the translation rates or protein stability of some important factors, thereby promoting diet-induced metabolic disorders. For example, inflammation and free fatty acid (FFA)-triggered JNK activation caused the ubiquitination and proteasomal degradation of cellular FADD-like apoptosis regulator (c-FLIPL), which exacerbates cell death of hepatocytes and nonalcoholic steatohepatitis (NASH) [10]. Small ubiquitin-related modifier (SUMO)—specific protease 2 (SENP2) expression was increased in HFD-induced fatty liver. SENP2 interacted with peroxisome proliferator-activated receptor-α (PPARα) and deSUMOylated it, thereby promoting ubiquitylation and subsequent degradation of PPARα, which in turn result in aggravated liver steatosis [22]. Given that SERPINA3C expression was inhibited at the protein level but not the mRNA level, it is likely HFD-feeding may trigger some stress signals to suppress the expression of SERPINA3C through an effect after transcription, such as by promoting the protein degradation of SERPINA3C, which merits further investigation.

Our results suggest that SERPINA3C-mediated inhibition of inflammation in adipocytes improved insulin sensitivity and oxygen consumption of adipose tissue. In the HFD-fed mice, SERPINA3C deficiency also led to impaired insulin sensitivity and oxygen consumption in the brown adipose tissue (BAT), liver, and muscle (Supplementary Figure 4L-Q; Supplementary Figure 3C). However, the inflammation levels in the abovementioned three tissues were only slightly affected by knockout of SERPINA3C (Supplementary Figs. 4A—I). Adipose tissue is an important metabolic tissue for regulating glucose homeostasis. SERPINA3C deficiency damaged insulin sensitivity in adipose tissues, which further led to systemic dysregulation of glucose metabolism, thereby elevating blood glucose levels. High glucose is toxic and impairs mitochondrial function to inhibit mitochondrial respiration in the BAT, liver, and muscle. Inflammation of adipose tissue also influences the metabolic homeostasis of lipids in adipose tissue, which alters lipid contents in the circulation. This may lead to lipotoxicity that could further impair insulin sensitivity and mitochondrial function of cells in other metabolic organs [41]. Similarly, localized overexpression of SERPINA3C in iWAT improved insulin sensitivity and oxygen consumption in the BAT, liver and muscle (Supplementary Figs. 7F—K; Supplementary Figure 6C), whose inflammation levels were only mildly decreased by iWAT overexpression of SERPINA3C. This may be explained by the decreased blood glucose and lipotoxicity. Thus, our data suggest that SERPINA3C promoted metabolic homeostasis in adipose tissue by attenuating the inflammation of adipocytes, which may play an important role in improving insulin sensitivity and mitochondrial function of metabolic organs, including adipose tissue, liver, and muscle, thereby systematically ameliorating DIO-associated metabolic disorders in mice.

Glut2 is the major glucose transporter in hepatocytes and mediate mainly the basal glucose uptake [42]. However, a number of studies have reported that insulin can indeed stimulate the uptake of glucose/2-DG by the liver/hepatocytes. Insulin treatment (100 nM, 20 min) obviously stimulated 2-NBDG uptake in HepG2 cells (50% increase relative to baseline) and Huh7 cells (40% increase relative to baseline), both are human hepatocellular carcinoma cell lines [43]. Insulin (100 nM) also promoted 2-DG uptake by HepG2 (increased about 30% relative to baseline) in another independent study [44]. These above two studies were conducted in hepatocyte cell lines and they both demonstrate that insulin can promote 2-DG uptake of hepatocytes. In 2011, a work published in Nature Medicine showed that insulin (20 ng/mL, 15 min) significantly stimulated ^{3}H-D-glucose uptake (250% increase relative to baseline) in primary cultures of mice hepatocytes [45]. Moreover, research aimed to measure ex vivo tissue-specific glucose uptake (liver, soleus, and WATs) also showed that insulin (10 mU/ml, 15 min) significantly increased 2-DG uptake by 37% in the liver [46]. In our study, we found that insulin stimulated 2-DG uptake of mice liver (30% increase relative to baseline as shown in Supplementary Figure 4P, and Supplementary Figure 7J), which was consistent with previous works. All these studies above indicate that there exists insulin-dependent glucose/2-DG uptake in liver/hepatocytes. Further studies are needed to investigate the mechanism underlying insulin-stimulated glucose uptake of hepatocytes.

Cathepsin G belongs to the neutrophil serine proteases family, known for its function in killing pathogens. Cathepsin G has important effects on inflammation and immune reactions [47]. Cathepsin G has the ability to cleave and activate IL-36γ and aggravate imiquimod-induced mouse psoriatic lesions [48]. Intracardiac administration of Cathepsin G promotes inflammation and pathological remodeling in the non-injured heart [49]. However, most of these studies concentrated on non-adipose tissues. A recent study reported that knockdown of SERPINA3C in preadipocytes led to increased Cathepsin G activity [18], but this was conducted in undifferentiated preadipocytes *in vitro*. Our study is the first to define the increased activity of Cathepsin G in the adipose tissue of obese mice, which suggest that Cathepsin G may regulate inflammation in mature adipocytes and adipose tissue. We found aggravated inflammation in SERPINA3C—KO mice with enhanced Cathepsin G activity. While the level of inflammation was decreased when SERPINA3C was overexpressed in iWAT, which was associated with reduced Cathepsin G activity. This supports the notion that Cathepsin G activity was a key downstream target of SERPINA3C in ameliorating adipose tissue inflammation. Therefore, a previously unknown adipose SERPINA3C/Cathepsin G axis was identified in our study, which plays an important role in regulating adipose tissue inflammation and metabolic homeostasis.

Integrins are heterodimers containing transmembrane α and β subunits, which regulate the development, immunity and inflammation [36,50]. Integrins were important effectors in adipose metabolism [51—54]. In our study, α5 and β1 Integrin protein levels were decreased when SERPINA3C was ablated, but SERPINA3C overexpression increased α5 and β1 Integrin protein levels. As transmembrane heterodimers, integrins could be the intermediary agents between extracellular SERPINA3C-mediated inhibition of Cathepsin G and intracellular AKT activation and JNK suppression. We

demonstrated that Cathepsin G decreased α5/β1 Integrin protein expression levels. Furthermore, SERPINA3C abolished the Cathepsin G-mediated decline of α5/β1 Integrin proteins to inhibit inflammation in adipocytes. Together, these results suggest that α5/β1 Integrin signaling could be the critical mediator of SERPINA3C/Cathepsin G axis in the inhibition of adipocyte inflammation.

In summary, we identified a previously less-known adipokine that regulates adipose tissue homeostasis and systemic metabolism in obese mice. We also identified SERPINA3C/Cathepsin G axis as an important regulatory signaling involved in the suppression of adipose tissue inflammation. Thus, the SERPINA3C/Cathepsin G/Integrin/AKT pathway in adipose tissue might be a potential therapeutic target for type 2 diabetes and obesity complications.

AUTHOR CONTRIBUTION STATEMENT

B.-Y.L. and L.G. were involved in study design, conducted the experiments, analyzed the data and drafted the paper; Y.-Y.G., and G.X. performed the experiments; L.G. and Q.-Q.T. designed, supervised the study and wrote the paper.

DATA AVAILABILITY

The data sets generated and/or analyzed during the current study are available from the corresponding author on reasonable request.

ACKNOWLEDGMENTS

We thank S. Cai from Department of Pathology of School of Basic Medical Sciences, Fudan University for assistance with images acquiring with Confocal Laser Scanning Microscopy (Leica). Dr. Q.-Q.T. is the guarantor of this work and, as such, had full access to all the data in the study and takes responsibility for the integrity of the data and the accuracy of the data analysis. This study was supported by the National Key R&D Program of the Ministry of Science and Technology of China (2018YFA0800401) to Q.-Q.T., National Natural Science Foundation (NSFC) grants (31871435 and 32070751 to L.G., 81730021 and 32070760 to Q.-Q.T).

CONFLICT OF INTEREST

The authors have declared that no conflict of interest exists.

APPENDIX A. SUPPLEMENTARY DATA

Supplementary data to this article can be found online at https://doi.org/10.1016/j.molmet.2022.101500.

REFERENCES

[1] Ng, A.C.T., Delgado, V., Borlaug, B.A., Bax, J.J., 2021. Diabesity: the combined burden of obesity and diabetes on heart disease and the role of imaging. Nature Reviews Cardiology 18:291–304.

[2] Luk, C.T., Shi, S.Y., Cai, E.P., Sivasubramaniyam, T., Krishnamurthy, M., Brunt, J.J., et al., 2017. FAK signalling controls insulin sensitivity through regulation of adipocyte survival. Nature Communications 8:14360.

[3] Guo, Y.Y., Li, B.Y., Peng, W.Q., Guo, L., Tang, Q.Q., 2019. Taurine-mediated browning of white adipose tissue is involved in its anti-obesity effect in mice. Journal of Biological Chemistry 294:15014–15024.

[4] Peng, W.Q., Xiao, G., Li, B.Y., Guo, Y.Y., Guo, L., Tang, Q.Q., 2021. l-Theanine activates the browning of white adipose tissue through the AMPK/alpha-Ketoglutarate/Prdm16 Axis and ameliorates diet-induced obesity in mice. Diabetes 70:1458–1472.

[5] Chen, M., Zhu, J.-Y., Mu, W.-J., Guo, L., 2022. Cysteine dioxygenase type 1 (CDO1): its functional role in physiological and pathophysiological processes. Genes & Diseases.

[6] Guo, S., Huang, Y., Zhang, Y., Huang, H., Hong, S., Liu, T., 2020. Impacts of exercise interventions on different diseases and organ functions in mice. Journal Sport Health Science 9:53–73.

[7] Luan, X., Tian, X., Zhang, H., Huang, R., Li, N., Chen, P., et al., 2019. Exercise as a prescription for patients with various diseases. Journal Sport Health Science 8:422–441.

[8] Mu, W.J., Zhu, J.Y., Chen, M., Guo, L., 2021. Exercise-mediated browning of white adipose tissue: its significance, mechanism and effectiveness. International Journal of Molecular Sciences 22.

[9] Wang, R., Tian, H., Guo, D., Tian, Q., Yao, T., Kong, X., 2020. Impacts of exercise intervention on various diseases in rats. Journal Sport Health Science 9:211–227.

[10] Guo, L., Zhang, P., Chen, Z., Xia, H., Li, S., Zhang, Y., et al., 2017. Hepatic neuregulin 4 signaling defines an endocrine checkpoint for steatosis-to-NASH progression. Journal of Clinical Investigation 127:4449–4461.

[11] Kershaw, E.E., Flier, J.S., 2004. Adipose tissue as an endocrine organ. Journal of Clinical Endocrinology & Metabolism 89:2548–2556.

[12] Scheja, L., Heeren, J., 2019. The endocrine function of adipose tissues in health and cardiometabolic disease. Nature Reviews Endocrinology 15:507–524.

[13] Law, R.H., Zhang, Q., McGowan, S., Buckle, A.M., Silverman, G.A., Wong, W., et al., 2006. An overview of the serpin superfamily. Genome Biology 7:216.

[14] Spence, M.A., Mortimer, M.D., Buckle, A.M., Minh, B.Q., Jackson, C.J., 2021. A comprehensive phylogenetic analysis of the serpin superfamily. Molecular Biology and Evolution 38:2915–2929.

[15] Irving, J.A., Pike, R.N., Lesk, A.M., Whisstock, J.C., 2000. Phylogeny of the serpin superfamily: implications of patterns of amino acid conservation for structure and function. Genome Research 10:1845–1864.

[16] Gagaoua, M., Hafid, K., Boudida, Y., Becila, S., Ouali, A., Picard, B., et al., 2015. Caspases and thrombin activity regulation by specific serpin inhibitors in bovine skeletal muscle. Applied Biochemistry and Biotechnology 177:279–303.

[17] Schick, C., G.P. Pemberton Pa Fau - Shi, Y. Shi Gp Fau - Kamachi, S. Kamachi Y Fau - Cataltepe, A.J. Cataltepe S Fau - Bartuski, E.R. Bartuski Aj Fau - Gornstein, et al, Cross-class inhibition of the cysteine proteinases cathepsins K, L, and S by the serpin squamous cell carcinoma antigen 1: a kinetic analysis.

[18] Choi, Y., Choi, H., Yoon, B.K., Lee, H., Seok, J.W., Kim, H.J., et al., 2020. Serpina3c regulates adipogenesis by modulating insulin growth factor 1 and integrin signaling. iScience 23:100961.

[19] Qian, L.L., Ji, J.J., Guo, J.Q., Wu, Y.P., Ma, G.S., Yao, Y.Y., 2021. Protective role of serpina3c as a novel thrombin inhibitor against atherosclerosis in mice. Clinical Science 135:447–463.

[20] Ji, J.J., Qian, L.L., Zhu, Y., Wu, Y.P., Guo, J.Q., Ma, G.S., et al., 2020. Serpina3c protects against high-fat diet-induced pancreatic dysfunction through the JNK-related pathway. Cellular Signalling 75:109745.

[21] Liu, Y., Peng, W.Q., Guo, Y.Y., Liu, Y., Tang, Q.Q., Guo, L., 2018. Kruppel-like factor 10 (KLF10) is transactivated by the transcription factor C/EBPbeta and involved in early 3T3-L1 preadipocyte differentiation. Journal of Biological Chemistry 293:14012–14021.

[22] Liu, Y., Dou, X., Zhou, W.Y., Ding, M., Liu, L., Du, R.Q., et al., 2021. Hepatic small ubiquitin-related modifier (SUMO)-Specific protease 2 controls systemic metabolism through SUMOylation-dependent regulation of liver-adipose tissue crosstalk. Hepatology 74:1864–1883.

[23] Guo, L., Guo, Y.Y., Li, B.Y., Peng, W.Q., Chang, X.X., Gao, X., et al., 2019. Enhanced acetylation of ATP-citrate lyase promotes the progression of nonalcoholic fatty liver disease. Journal of Biological Chemistry 294:11805–11816.

[24] Guo, L., Zhou, S.R., Wei, X.B., Liu, Y., Chang, X.X., Liu, Y., et al., 2016. Acetylation of mitochondrial trifunctional protein alpha-subunit enhances its stability to promote fatty acid oxidation and is decreased in nonalcoholic fatty liver disease. Molecular and Cellular Biology 36:2553–2567.
[25] Guo, L., Guo, Y.Y., Li, B.Y., Peng, W.Q., Tang, Q.Q., 2019. Histone demethylase KDM5A is transactivated by the transcription factor C/EBPbeta and promotes preadipocyte differentiation by inhibiting Wnt/beta-catenin signaling. Journal of Biological Chemistry 294:9642–9654.
[26] Wang, G.X., Zhao, X.Y., Meng, Z.X., Kern, M., Dietrich, A., Chen, Z., et al., 2014. The brown fat-enriched secreted factor Nrg4 preserves metabolic homeostasis through attenuation of hepatic lipogenesis. Natural Medicine 20: 1436–1443.
[27] Guilherme, A., Virbasius, J.V., Puri, V., Czech, M.P., 2008. Adipocyte dysfunctions linking obesity to insulin resistance and type 2 diabetes. Nature Reviews Molecular Cell Biology 9:367–377.
[28] Wellen, K.E., Hotamisligil, G.S., 2003. Obesity-induced inflammatory changes in adipose tissue. Journal of Clinical Investigation 112:1785–1788.
[29] Sun, X., Seidman, J.S., Zhao, P., Troutman, T.D., Spann, N.J., Que, X., et al., 2020. Neutralization of oxidized phospholipids ameliorates non-alcoholic steatohepatitis. Cell Metabolism 31:189–206 e8.
[30] Solinas, G., Becattini, B., 2017. JNK at the crossroad of obesity, insulin resistance, and cell stress response. Molecular Metabolism 6:174–184.
[31] Hou, S., Jiao, Y., Yuan, Q., Zhai, J., Tian, T., Sun, K., et al., 2018. S100A4 protects mice from high-fat diet-induced obesity and inflammation. Laboratory Investigation 98:1025–1038.
[32] Cheng, Y., Buchan, M., Vitanova, K., Aitken, L., Gunn-Moore, F.J., Ramsay, R.R., et al., 2020. Neuroprotective actions of leptin facilitated through balancing mitochondrial morphology and improving mitochondrial function. Journal of Neurochemistry 155:191–206.
[33] Kriszt, R., Arai, S., Itoh, H., Lee, M.H., Goralczyk, A.G., Ang, X.M., et al., 2017. Optical visualisation of thermogenesis in stimulated single-cell brown adipocytes. Scientific Reports 7:1383.
[34] van Horssen, J., van Schaik, P., Witte, M., 2019. Inflammation and mitochondrial dysfunction: a vicious circle in neurodegenerative disorders? Neuroscience Letters 710:132931.
[35] Pidard, D., Renesto, P., Berndt, M.C., Rabhi, S., Clemetson, K.J., Chignard, M., 1994. Neutrophil proteinase cathepsin G is proteolytically active on the human platelet glycoprotein Ib-IX receptor: characterization of the cleavage sites within the glycoprotein Ibα subunit. Biochemical Journal 303:489–498.
[36] Shattil, S.J., Kim, C., Ginsberg, M.H., 2010. The final steps of integrin activation: the end game. Nature Reviews Molecular Cell Biology 11:288–300.
[37] Streuli, C.H., 2016. Integrins as architects of cell behavior. Molecular Biology of the Cell 27:2885–2888.
[38] Ruiz-Ojeda, F.J., Mendez-Gutierrez, A., Aguilera, C.M., Plaza-Diaz, J., 2019. Extracellular matrix remodeling of adipose tissue in obesity and metabolic diseases. International Journal of Molecular Sciences 20.
[39] Heemskerk, J.W., Mattheij, N.J., Cosemans, J.M., 2013. Platelet-based coagulation: different populations, different functions. Journal of Thrombosis and Haemostasis 11:2–16.
[40] Zong, H., Bastie, C.C., Xu, J., Fassler, R., Campbell, K.P., Kurland, I.J., et al., 2009. Insulin resistance in striated muscle-specific integrin receptor beta1-deficient mice. Journal of Biological Chemistry 284:4679–4688.
[41] Slawik, M., Vidal-Puig, A.J., 2006. Lipotoxicity, overnutrition and energy metabolism in aging. Ageing Research Reviews 5:144–164.
[42] Leturque, A., Brot-Laroche, E., Le Gall, M., 2009. GLUT2 mutations, translocation, and receptor function in diet sugar managing. American Journal of Physiology. Endocrinology and Metabolism 296:E985–E992.
[43] Yang, C.P., Shiau, M.Y., Lai, Y.R., Ho, K.T., Hsiao, C.W., Chen, C.J., et al., 2018. Interleukin-4 boosts insulin-induced energy deposits by enhancing glucose uptake and lipogenesis in hepatocytes. Oxidative Medicine and Cellular Longevity 2018:6923187.
[44] De Toni, L., Di Nisio, A., Rocca, M.S., Guidolin, D., Della Marina, A., Bertazza, L., et al., 2021. Exposure to perfluoro-octanoic acid associated with upstream uncoupling of the insulin signaling in human hepatocyte cell line. Frontiers in Endocrinology 12:632927.
[45] Fafalios, A., Ma, J., Tan, X., Stoops, J., Luo, J., Defrances, M.C., et al., 2011. A hepatocyte growth factor receptor (Met)-insulin receptor hybrid governs hepatic glucose metabolism. Natural Medicine 17:1577–1584.
[46] Tavares, G., Martins, F.O., Melo, B.F., Matafome, P., Conde, S.V., 2021. Peripheral dopamine directly acts on insulin-sensitive tissues to regulate insulin signaling and metabolic function. Frontiers in Pharmacology 12: 713418.
[47] Gao, S., Zhu, H., Zuo, X., Luo, H., 2018. Cathepsin G and its role in inflammation and autoimmune diseases. Archives Rheumatology 33:498–504.
[48] Guo, J., Tu, J., Hu, Y., Song, G., Yin, Z., 2019. Cathepsin G cleaves and activates IL-36gamma and promotes the inflammation of psoriasis. Drug Design, Development and Therapy 13:581–588.
[49] Miller, S.A., Kolpakov, M.A., Guo, X., Du, B., Nguyen, Y., Wang, T., et al., 2019. Intracardiac administration of neutrophil protease cathepsin G activates non-canonical inflammasome pathway and promotes inflammation and pathological remodeling in non-injured heart. Journal of Molecular and Cellular Cardiology 134:29–39.
[50] Hynes, R.O., Integrins: bidirectional, allosteric signaling machines.
[51] Bugler-Lamb, A.R., Hasib, A., Weng, X., Hennayake, C.K., Lin, C., McCrimmon, R.J., et al., 2021. Adipocyte integrin-linked kinase plays a key role in the development of diet-induced adipose insulin resistance in male mice. Molecular Metabolism 49:101197.
[52] Kim, H., Wrann, C.D., Jedrychowski, M., Vidoni, S., Kitase, Y., Nagano, K., et al., 2018. Irisin mediates effects on bone and fat via alphaV integrin receptors. Cell 175:1756–1768 e17.
[53] Oguri, Y., Shinoda, K., Kim, H., Alba, D.L., Bolus, W.R., Wang, Q., et al., 2020. CD81 controls beige fat progenitor cell growth and energy balance via FAK signaling. Cell 182:563–577 e20.
[54] Ruiz-Ojeda, F.J., Wang, J., Backer, T., Krueger, M., Zamani, S., Rosowski, S., et al., 2021. Active integrins regulate white adipose tissue insulin sensitivity and brown fat thermogenesis. Molecular Metabolism 45: 101147.

